


METTL3-Mediated m⁶A Modification of lncRNA-0949 Drives Microglial Inflammation in an *in vitro* Model of Sepsis-Associated Encephalopathy

Xing Zeng*, Xiao-Juan Luo*, Zhen-Ze Zhang, Jia-Li Lu, Yi-An Zhan 

Department of Respiratory and Critical Care Medicine, The First Affiliated Hospital of Nanchang University, Nanchang, Jiangxi, 330006, People's Republic of China

*These authors contributed equally to this work

Correspondence: Yi-An Zhan, Department of Respiratory and Critical Care Medicine, The First Affiliated Hospital of Nanchang University, Nanchang, Jiangxi, 330006, People's Republic of China, Tel +86-18879100002, Email ndyf02169@ncu.edu.cn

Introduction: Sepsis-associated encephalopathy (SAE) is a severe complication of sepsis with limited therapeutic options. Although neuroinflammation driven by microglial activation is central to SAE pathogenesis, the underlying epitranscriptional regulatory mechanisms remain poorly defined. Here, we investigated the role of the m⁶A methyltransferase METTL3 in regulating microglial inflammation using lipopolysaccharide (LPS)-stimulated HMO6 microglial cells as an *in vitro* SAE model.

Methods: HMO6 cells were stimulated with LPS (1 µg/mL) for 0–24 h to establish an SAE model. METTL3 expression was assessed by Western blotting and immunofluorescence. MeRIP-qPCR was used to detect m⁶A deposition on lncRNA-0949. METTL3 was inhibited pharmacologically (3-DAA) or by siRNA knockdown. lncRNA-0949 stability was evaluated by actinomycin D chase assay. Luciferase reporters containing wild-type or m⁶A site-mutated lncRNA-0949 3'UTR were constructed to identify functional m⁶A sites. Wild-type and m⁶A site-mutated lncRNA-0949 overexpression vectors were employed to assess modification-dependent pro-inflammatory function. Cytokine mRNA (qRT-PCR) and protein (ELISA) levels were measured.

Results: LPS stimulation time-dependently increased oxidative stress (MDA), pro-inflammatory cytokines (MIP-2, IL-1β, TNF-α, IL-6), and METTL3 protein expression (2.99-fold at 24 h, *P* < 0.001). METTL3 catalyzed m⁶A deposition on lncRNA-0949, with enrichment reaching 21.3-fold at 24 h post-LPS (*P* < 0.001). METTL3 knockdown abolished this modification and reduced lncRNA-0949 stability, decreasing its half-life from ~30 h to 11 h (*P* < 0.001). The m⁶A site within the 3'UTR (RRACH motif) was essential for LPS-induced reporter activity (7.7-fold increase for WT vs. no response for Mut, *P* < 0.001). Overexpression of wild-type lncRNA-0949 amplified LPS-triggered cytokine release (eg, TNF-α increased by additional 33%, *P* < 0.001), whereas the m⁶A site mutant had no effect. Conversely, METTL3 knockdown attenuated LPS-induced inflammatory responses, with mRNA levels reduced by 35–58% and protein levels by 30–63% (all *P* < 0.001).

Conclusion: Together, these findings define a METTL3–m⁶A–lncRNA-0949 regulatory axis that amplifies microglial inflammation in an *in vitro* SAE model. This study provides the first evidence that METTL3-driven m⁶A modification of lncRNA-0949 contributes to neuroinflammation, offering a new mechanistic perspective and highlighting the need for *in vivo* validation to assess therapeutic potential.

Keywords: lncRNA-0949, septic encephalopathy, METTL3, inflammation

Introduction

Sepsis is a systemic inflammatory response caused by infection, which is the direct cause of death in critically ill patients in intensive care unit (ICU). In clinical practice, sepsis is mainly manifested by multiple organ dysfunction. Sepsis-associated encephalopathy is one of the common complications of sepsis, which is usually accompanied by acute neurological dysfunction, manifested as disturbance of consciousness, cognitive dysfunction, memory loss and other symptoms.¹ Uncontrolled severe inflammation in the brain is the main cause of SAE.² Microglia are the resident immune cells inherent in the central nervous system. When the CNS is injured or invaded by diseases, microglia will show complex responses and

release a series of pro-inflammatory cytokines, thereby inducing neuroinflammatory responses.^{3–5} Therefore, understanding the mechanisms of how microglia are aberrantly activated is key to developing effective therapies for SAE. Although neuroinflammatory response is the pathological mechanism leading to the development of SAE, its post-transcriptional regulatory mechanisms, particularly at the RNA epigenetic level, remain unclear. Therefore, this study aims to explore the role of RNA epigenetic modifications, specifically m⁶A, in microglial inflammation during SAE.

RNA epigenetic modifications such as m⁶A and m⁵C play an important role in regulating gene expression, cell function and inflammatory stress response.⁶ Among them, m⁶A (N⁶-methyladenosine) is the most important modification in mammalian mRNA and lncRNA.⁷ In the process of regulating the dynamic modification of m⁶A, methyltransferases, demethylases and recognition enzymes cooperated. The methyltransferase complex (such as METTL3/METTL14 heterodimer), as the core writing enzyme of m⁶A modification, exerted global regulation on RNA metabolism by catalyzing the methylation of adenosine at N⁶ position.⁸ Studies have shown that METTL3 is the key enzyme that catalyzes the methylation of m⁶A in RNA, and it plays an important role in regulating the immune inflammatory response caused by macrophages. It can regulate the activation and function of immune cells by binding to the methylation sites of RNA.^{9,10} Recent studies have found that METTL3 can directly affect the “lifetime” of long non-coding RNA (lncRNA) with the help of m⁶A methylation, which opens a new door to understand the upstream regulation of lncRNA.^{11,12} Moreover, m⁶A modifications are recognized by reader proteins such as IGF2BP2, which can influence RNA stability and function.¹³ However, the role of METTL3 in microglia, the resident immune cells of the brain, remains poorly understood.¹⁴

Long non-coding RNA (lncRNA) is a kind of linear non-coding RNA, which plays an important role in gene regulation.¹⁵ In recent years, lncRNAs have been found to be closely related to a variety of nervous system diseases and inflammatory responses, and their mechanisms involve transcriptional regulation, competing endogenous RNAs, and activation of related inflammasomes.^{16,17} lncRNA-0949, first identified in 2014,¹⁸ remains functionally uncharacterized. In our previous study, we observed its significant upregulation in LPS-treated iPSC-Exos co-incubated with HMO6 microglial cells ([Supplementary Figure 1A and B](#))—a model where iPSC-Exos reduced microglial inflammatory cytokines (TNF- α , IL-1 β , IL-6) upon LPS stimulation. This suggested a potential role for lncRNA-0949 in the anti-inflammatory effect of iPSC-Exos, prompting us to explore its function in microglial inflammation. Given that METTL3 can regulate lncRNA stability via m⁶A modification,^{19,20} we now ask whether METTL3 modifies lncRNA-0949 to regulate microglial inflammatory responses in the pathological context of SAE. This question is important because it links the chemical modification of RNA with the function of lncRNA and helps us to understand how neuroinflammation is regulated.

The core research hypothesis is that the expression of METTL3 is increased by inflammatory mediators under SAE conditions. The up-regulated METTL3 enhanced the stability of lncRNA-0949 via m⁶A modification, which ultimately aggravated neuroinflammation. To test this hypothesis, we constructed an in vitro model of LPS-activated human microglia (HMO6) to mimic the SAE environment by (1) confirming whether METTL3 is responsible for the m⁶A modification and stability of lncRNA-0949; (2) To investigate whether m⁶A modification is necessary for the pro-inflammatory function of lncRNA-0949; (3) to verify the central role of “METTL3-m⁶A-lncRNA-0949” in driving the inflammatory response of microglia. We aimed to uncover a novel epigenetic regulatory pathway in SAE and provide new targets for the pathogenesis and potential treatment of the sepsis-associated brain.

Materials and Methods

Cell Culture and Processing

HMO6 cells were purchased from Shanghai Enzyme-linked Biotechnology (cat# C1024) and cultured in DMEM (Hyclone, cat# SH30243.02) supplemented with 10% fetal bovine serum (FBS, Gibco) and 1% penicillin-streptomycin (PS, Hyclone, cat# SV30010) at 37°C in a 5% CO₂ humidified incubator. The culture medium was refreshed every 2–3 days. For LPS treatment, cells were seeded in 6-well plates at a density of 1×10⁵ cells per well, allowed to adhere overnight, and then stimulated with 1 μ g/mL lipopolysaccharide (LPS, from *Escherichia coli* O111:B4, Sigma, cat# L5293) dissolved in PBS for 0, 6, 12, or 24 h in DMEM (Hyclone, cat# SH30243.02) containing 1% FBS (Gibco). Control cells received an equivalent volume of PBS. All experiments were performed with at least three independent biological replicates.

MDA

MDA levels were measured using a commercial kit (S0131S; Beyotime, China) per manufacturer's instructions. Cells were lysed in PBS by sonication, centrifuged, and supernatants incubated with TBA working solution at 100°C for 15 min. After cooling and centrifugation, absorbance was read at 532 nm. MDA concentrations were calculated via a standard curve and normalized to protein content.

RNA m⁶A Quantification

Total m⁶A levels were measured using the EpiQuik m⁶A RNA Methylation Quantification Kit (Epigentek, cat# P-9005-48; distributed by Wuhan AmyJet Scientific, China) per manufacturer's instructions. Briefly, 200 ng of poly(A)-purified RNA was incubated with capture antibody, detection antibody, and enhancer solutions, and absorbance was read at 450 nm. m⁶A percentage was calculated using the kit's formula.

RT-qPCR

Total RNA was extracted from HMO6 cells using TRIzol (Invitrogen). RT-qPCR was performed with SYBR Green Master Mix (Thermo Fisher Scientific) on a QuantStudio 5 system. Relative mRNA expression was calculated by the $2^{-\Delta\Delta Ct}^{21}$ method with GAPDH as internal control. Primers were designed and synthesized by GenePharma (Shanghai, China). Primer sequences are listed in Table 1.

Me-RIP

MeRIP was performed using a commercial kit (Junli Biology, GK-4043). Briefly, 100 µg of RNA was fragmented to ~200 nt (70°C, 6 min). Ten percent was saved as input; the remaining RNA was immunoprecipitated with anti-m⁶A antibody (Abcam, ab151230) at 4°C for 3 h. After washing, bound RNA was eluted and analyzed by RT-qPCR with lncRNA-0949-specific primers (Table 1). m⁶A enrichment was calculated as %input following the kit manual.

Immunofluorescence

HMO6 cells on coverslips were fixed, permeabilized, blocked, and incubated with rabbit anti-METTL3 (1:400; 10761-1-AP; Proteintech) and rabbit anti-IGF2BP2 (1:400; 11601-1-AP; Proteintech) at 4°C overnight. After washing, cells were incubated with Alexa Fluor 488 goat anti-rabbit IgG (1:1000; SA00013-2; Proteintech) or Alexa Fluor 555 goat anti-rabbit IgG (1:50; SA00013-4; Proteintech) for 90 min at room temperature. Nuclei were counterstained with DAPI. Fluorescence images were captured using a fluorescence microscope. All experiments were performed with three independent replicates.

Table 1 Primer Sequences of Each Gene

Gene	Primer Sequence (5'→3')
TNF-α	Forward: CAGGGGCCACACGCTCTTC Reverse: CTTGGGGCAGGGGCTCTTGA
IL-6	Forward: ATGAACTCCTTCTCCACAAGCGC Reverse: GAAGAGCCCTCAGGCTGGACTG
IL-1β	Forward: TCCCTTCATCTTTGAAGAAGA Reverse: GAGGCCCAAGGCCACAGG
MIP-2	Forward: TCCAAGAAAGGGCGAAATAAGG Reverse: TGCAGCTCTATCTGAATGTCTGT
GAPDH	Forward: TGTGGATGGCCCTCTGGAA Reverse: TGACCTTGCCACAGCCTTG

siRNA Transfection

The siRNA targeting human METTL3 (sense strand: 5'-GGAGAUCCUAGAGCUAUUA-3'; antisense strand: 5'-CCUCUAGGAUCUCGAUAAU-3') was designed based on a previously validated sequence²² and synthesized by GenePharma (Shanghai, China). HMO6 cells were seeded in culture plates and transfected upon reaching 70–80% confluence. According to the manufacturer's instructions, cells were transfected with either siMETTL3 (experimental group) or negative control siRNA (control group) using siRNA-Mate plus transfection reagent (GenePharma, Cat. No. G04002). Cells were harvested 48–72 hours post-transfection for subsequent experiments.

Western Blot

Cells were lysed in RIPA buffer (Roche). Protein concentration was determined by BCA assay (Beyotime). Equal protein (50 µg) was resolved by 12% SDS-PAGE, transferred to PVDF membranes, blocked with 5% skim milk, and incubated with primary antibodies (anti-METTL3 ab195352 1:1000, anti-IGF2BP2 ab128175 1:1500, anti-GAPDH ab9485 1:5000; Abcam) overnight at 4°C, followed by HRP-conjugated goat anti-rabbit secondary antibody (ab6721 1:6000; Abcam) for 1 h. Bands were visualized by ECL (Beyotime) and quantified using Quantity One (Bio-Rad) with GAPDH as loading control.

ELISA

Cell culture supernatants were collected and centrifuged. Levels of TNF- α (88–7346-22), IL-1 β (88–7261-22), IL-6 (88–7066-22), and MIP-2 (900-K120) were measured using human-specific ELISA kits (Thermo Scientific, USA) according to the manufacturer's protocols. Briefly, samples were added to pre-coated plates, incubated with detection antibody, and developed with TMB substrate. Absorbance was read at 450 nm, and cytokine concentrations were calculated from standard curves.

DB Experiment

RNA samples from control and LPS-treated cells (0,6,12,24 h) were serially diluted (1000–250 ng/µL), denatured (70°C, 5 min), and spotted (2 µL per dot) onto Hybond-N+ membrane (Cytiva, cat# RPN303B) in duplicate for m⁶A detection and methylene blue staining. After UV-crosslinking, membranes were blocked and incubated with anti-m⁶A antibody (Abcam, cat# ab151230, 1:1000), followed by HRP-conjugated secondary antibody. Signals were detected by ECL (Beyotime, cat# P0018AS) and quantified by densitometry. Relative m⁶A enrichment was calculated as fold change vs. the corresponding control at each time point. Methylene blue (Sigma Aldrich, cat# M9140) staining served as loading control. All experiments were performed with three independent biological replicates.

RNA Stability Assay

Cells transduced with METTL3 shRNA or control shRNA (referred to as siMETTL3 and siCtrl) were either left untreated or stimulated with LPS for 24 h. After actinomycin D (5 µg/mL) treatment, total RNA was collected at 0, 6, 12, and 24 h. lncRNA-0949 levels were quantified by RT-qPCR (GAPDH as internal control, 2⁻ $\Delta\Delta$ Ct method), and half-life was calculated from decay curves.

Luciferase Reporter Assay

The wild-type (WT) lncRNA-0949 3'UTR and its m⁶A site-mutated (mut, GGACA→GGCCA) sequence were cloned into the pmirGLO vector (Wuhan MiaoLing Biotechnology). HMO6 cells were co-transfected with the indicated reporter constructs and siRNAs, then stimulated with LPS. Luciferase activities were measured using the Dual-Luciferase Reporter Assay System (Beyotime). Firefly luciferase activity was normalized to Renilla luciferase activity.²³

Statistical Methods

All data are presented as mean \pm standard error of the mean (SEM) from at least three independent biological replicates, each performed with three technical replicates. Statistical analyses were conducted using GraphPad Prism (version 9.0). Normality was assessed using the Shapiro–Wilk test, and homogeneity of variances was verified by the Brown–Forsythe

test; all datasets met the assumptions for parametric testing. For comparisons between two groups, an unpaired two-tailed Student's *t*-test was used. For multiple group comparisons, one-way or two-way analysis of variance (ANOVA) was applied as appropriate, followed by Tukey's or Šidák's post hoc test for multiple comparisons. Statistical significance was defined as *** $P < 0.001$.

Results

LPS Time-Dependently Activates Microglia and Upregulates the Core Methyltransferase METTL3

To establish an LPS-stimulated human microglial (HMO6) model recapitulating key aspects of sepsis-associated encephalopathy (SAE), we challenged cells with lipopolysaccharide (LPS; 1 $\mu\text{g}/\text{mL}$) and assessed the pathogenic cascade over 0, 6, 12, and 24 h. Neuroinflammatory activation was confirmed by a significant rise in the oxidative stress marker malondialdehyde (MDA). LPS stimulation significantly increased MDA levels in a time-dependent manner (Figure 1A). Compared to control cells, MDA levels in LPS-treated cells were elevated at 6 h (0.64 ± 0.12 vs. 0.29 ± 0.12 , 2.2-fold, $P = 0.01$), 12 h (1.59 ± 0.12 vs. 0.25 ± 0.12 , 6.3-fold, $P < 0.001$), and 24 h (2.23 ± 0.12 vs. 0.29 ± 0.12 , 7.7-fold, $P < 0.001$). Transcript levels of the pro-inflammatory mediators MIP-2, IL-1 β , TNF- α , and IL-6 increased significantly in a time-dependent manner following LPS stimulation ($P < 0.001$ for both time and treatment effects; Figure 1B), a pattern corroborated at the protein level by ELISA (eg, TNF- α reached 305.6 pg/mL at 24 h vs. 26.5 pg/mL in controls, $P < 0.001$; Figure 1C). This shift to a pro-inflammatory phenotype prompted an investigation of upstream epitranscriptomic regulation. Given our prior transcriptomic data implicating lncRNA-0949 in SAE-relevant contexts (Supplementary Figure 1A and B), we analyzed the core N⁶-methyladenosine (m⁶A) methyltransferase METTL3. Western blotting revealed progressive accumulation of METTL3 protein throughout LPS stimulation (2.99 \pm 0.19-fold increase at 24 h vs. 0 h, $P < 0.001$; Figure 1D), a finding localized to the cell via intensified immunofluorescence signal at 24 h (Figure 1E). Collectively, these data position the sustained upregulation of METTL3 as a concomitant feature of evolving neuroinflammation in this cellular model.

LPS Induces Specific m⁶A Hypermethylation of lncRNA-0949 Through METTL3

Having established LPS-driven METTL3 upregulation, we next asked whether this activity directly targets lncRNA-0949. MeRIP-qPCR using an anti-m⁶A antibody was performed on RNA isolated from HMO6 cells at 0, 6, 12, and 24 h after LPS treatment. LPS stimulation led to a time-dependent increase in m⁶A enrichment on lncRNA-0949. Compared to control cells at the same time point, m⁶A levels in LPS-treated cells were significantly elevated at 6 h (0.85 ± 0.14 vs. 0.25 ± 0.14 , 3.4-fold, $P < 0.001$), 12 h (3.42 ± 0.14 vs. 0.25 ± 0.14 , 13.5-fold, $P < 0.001$), and 24 h (5.37 ± 0.14 vs. 0.25 ± 0.14 , 21.3-fold, $P < 0.001$; Figure 2A). A concomitant screen of m⁶A regulatory factors identified parallel upregulation of METTL3 mRNA (6.1-fold increase at 24 h vs. 0 h, Supplementary Figure 2A), pinpointing a coherent regulatory axis.

To establish METTL3 as the necessary writer, we inhibited its catalytic function pharmacologically with 3-deazadenosine (3-DAA) or knocked down the transcript with specific siRNA. The efficiency of METTL3 knockdown was confirmed by the complete loss of LPS-induced m⁶A enrichment on lncRNA-0949 (Figure 2C), which serves as a functional readout of effective silencing. Both interventions significantly attenuated the LPS-induced m⁶A enrichment on lncRNA-0949 at 24 h ($P < 0.001$ vs. LPS alone for both 3-DAA and siMETTL3; Figure 2B and C), a reversal corroborated by dot blot analysis (Supplementary Figure 2B). Thus, in LPS-stimulated HMO6 cells, inflammatory signalling co-opts the METTL3 methyltransferase to selectively deposit m⁶A marks on lncRNA-0949.

METTL3 Regulates the RNA Stability of lncRNA-0949 Through Its Specific m⁶A Site

We first assessed whether METTL3-mediated m⁶A deposition affects lncRNA-0949 stability. Following actinomycin D treatment to block transcription, the decay of lncRNA-0949 was monitored over 0, 6, 12, and 24 h by qRT-PCR with GAPDH as an internal control (the Ct values of GAPDH remained stable across all time points, variation < 0.5 cycles). HMO6 cells were divided into four groups: control (siNC, untreated), LPS (siNC + LPS), control+siMETTL3 (siMETTL3, untreated), and LPS+siMETTL3 (siMETTL3 + LPS). METTL3 knockdown significantly accelerated the

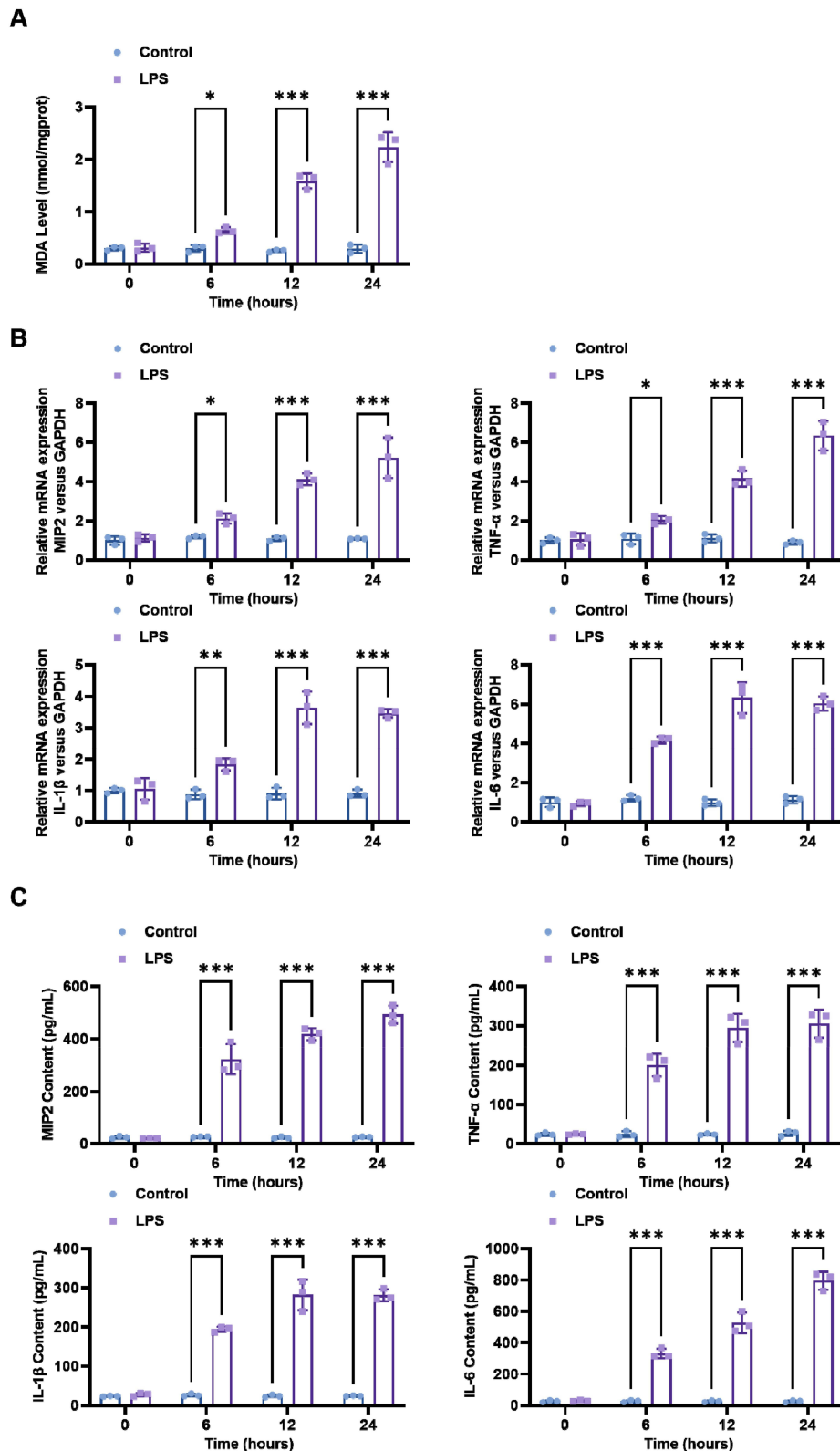


Figure 1 LPS activates microglia and upregulates METTL3 protein. HMO6 cells were stimulated with LPS (1 μg/mL) for 0, 6, 12, and 24 h, with untreated cells serving as controls. **(A)** Intracellular MDA levels were determined using the TBA method. **(B)** The mRNA expression of pro-inflammatory cytokines (MIP-2, IL-1β, TNF-α, IL-6) was quantified by RT-qPCR. **(C)** The secretion of the corresponding cytokines into the supernatant was measured by ELISA. **(D)** METTL3 protein expression was analyzed via Western blot, with representative blots and densitometric quantification shown. **(E)** Immunofluorescence staining for METTL3 (red) was performed; nuclei were stained with DAPI (blue). Representative images at 24 h are presented. Scale bar: 5 μm. Data represent the mean ± SD from three independent experiments (n = 3). Statistical significance was determined by two-way ANOVA followed by Sidák's multiple comparisons test. Asterisks denote statistical significance (*P < 0.05, **P < 0.01, ***P < 0.001).

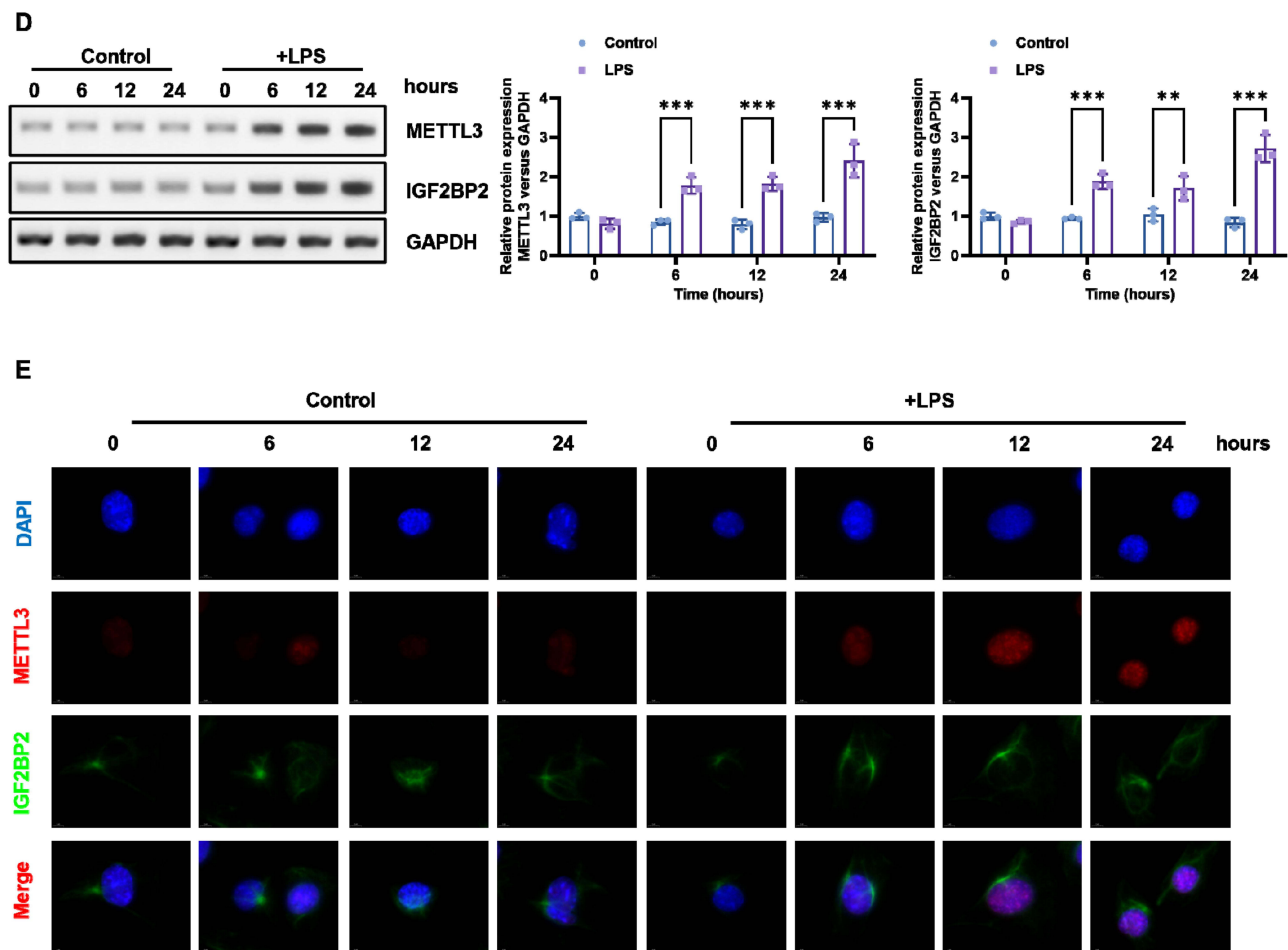


Figure 1 continued.

decay of lncRNA-0949 compared to the scrambled siRNA control. The estimated half-life of lncRNA-0949 was reduced from approximately 30 hours in control cells to 11 hours in METTL3-deficient cells ($P < 0.001$; Figure 3A).

To pinpoint the responsible cis-element, we engineered luciferase reporters bearing the lncRNA-0949 3'UTR, either wild-type (WT) or with a mutated core RRACH motif (mut), using the pmirGLO dual-luciferase vector, which expresses both firefly and Renilla luciferases from a single construct. HMO6 cells were transfected with each reporter along with siNC or siMETTL3 as indicated. Firefly luciferase activity was normalized to Renilla activity to control for transfection efficiency, and then expressed as fold change relative to the untreated control group. LPS stimulation significantly increased the activity of the WT reporter (approximately 7.7-fold vs. control, $P < 0.001$), while this increase was completely abolished by METTL3 knockdown ($P < 0.001$; Figure 3B). In contrast, the Mut reporter showed no response to LPS or METTL3 depletion (all $P > 0.05$ vs. control; Figure 3B). These results indicate that, in this LPS-stimulated microglial model, the METTL3-dependent m⁶A modification at the 3'UTR is essential for the LPS-induced increase in lncRNA-0949 activity, establishing that METTL3 regulates lncRNA-0949 abundance primarily via this specific m⁶A site.

The Pro-Inflammatory Function of lncRNA-0949 Strictly Depends on Its m⁶A Modification Status

To determine the functional consequence of this epitranscriptomic mark, we tested the pro-inflammatory activity of lncRNA-0949 in its m⁶A-modified versus unmodified states. Cells were transfected with wild-type (OE-WT) or m⁶A site-mutated (OE-Mut) lncRNA-0949 overexpression vectors and then left untreated or stimulated with LPS.

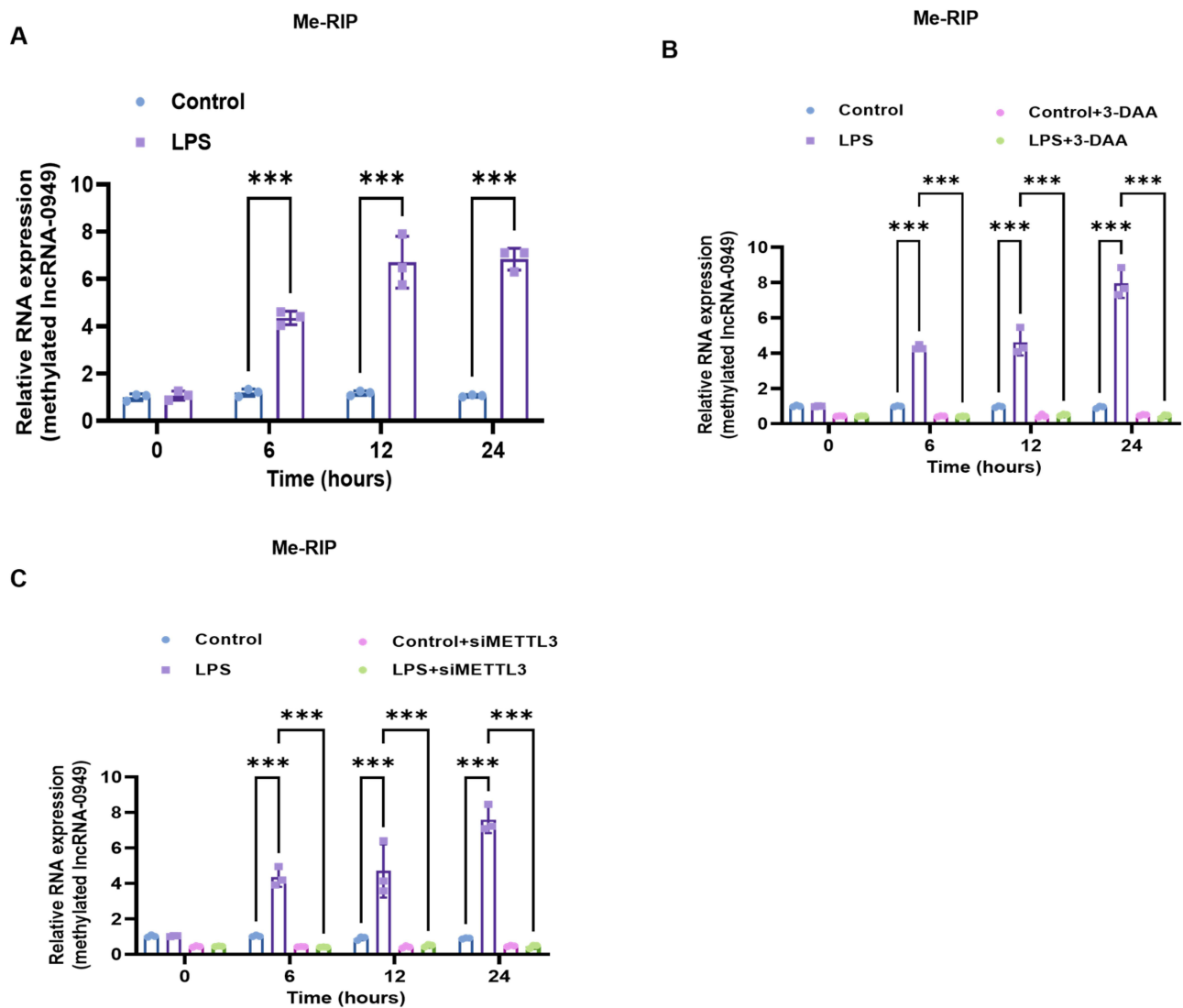


Figure 2 LPS induces METTL3-mediated m⁶A hypermethylation of lncRNA-0949. MeRIP-qPCR analysis of m⁶A enrichment on lncRNA-0949 in HMO6 cells at 0, 6, 12, and 24 h. **(A)** Time course of m⁶A levels in control and LPS-treated cells. **(B)** Effect of the m⁶A methyltransferase inhibitor 3-DAA on LPS-induced m⁶A modification. Cells were pretreated with 3-DAA prior to LPS stimulation. **(C)** Effect of METTL3 knockdown on LPS-induced m⁶A modification. Cells were transfected with control siRNA (siNC) or METTL3 siRNA (siMETTL3) and then left untreated or stimulated with LPS. Data are presented as mean \pm SD from three independent biological replicates ($n = 3$). For **(A)**, statistical significance was determined by two-way ANOVA followed by Šidák's multiple comparisons test. For **(B)** and **(C)**, statistical significance was determined by two-way ANOVA followed by Tukey's post hoc test. Asterisks denote statistical significance (***) ($P < 0.001$).

Overexpression of wild-type lncRNA-0949 amplified LPS-triggered release of pro-inflammatory cytokines at 24 h compared to the LPS alone group (eg, TNF- α increased by an additional 33%, $P < 0.001$; [Figure 4A](#) and [B](#)) and elevated oxidative stress ([Supplementary Figure 3A](#)). In contrast, overexpression of the m⁶A site mutant produced no such enhancement ($P > 0.05$ vs. LPS alone), demonstrating that the RNA's pro-inflammatory function in this context requires its specific modification, not simply its overexpression ([Figure 4A](#) and [B](#), [Supplementary Figure 3A](#)).

To position lncRNA-0949 as a functional effector within the METTL3–m⁶A pathway, we intervened upstream. METTL3 knockdown significantly attenuated LPS-induced inflammatory responses at 24 h, with mRNA levels reduced by approximately 35–58% ([Figure 4C](#)) and protein levels reduced by approximately 30–63% ([Figure 4D](#)) compared to the LPS + siNC group (all $P < 0.001$) and associated oxidative stress ([Supplementary Figure 3A](#)). Collectively, these findings delineate a METTL3–m⁶A–lncRNA-0949 regulatory axis in LPS-stimulated HMO6 microglia: inflammatory signalling induces METTL3, which stabilizes lncRNA-0949 via site-specific m⁶A deposition. The m⁶A-modified transcript in turn contributes to a pro-inflammatory program, mirroring features of the dysregulated microglial activation associated with SAE.

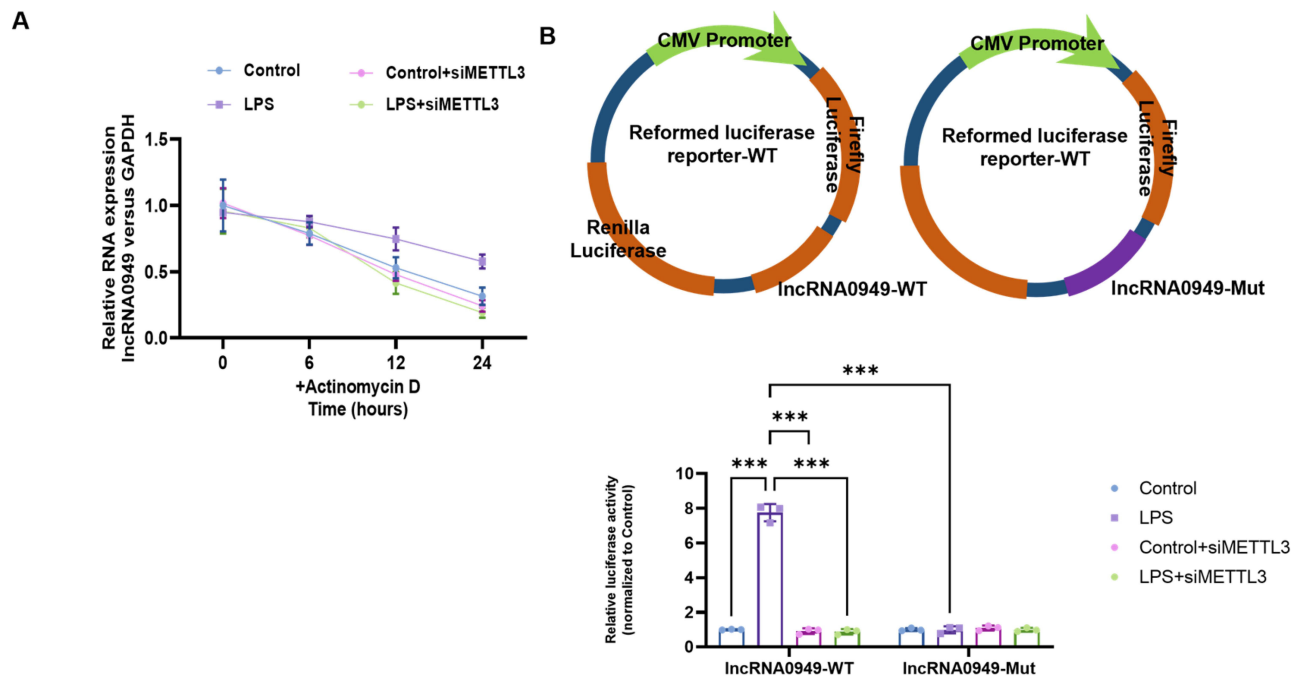


Figure 3 METTL3 regulates the RNA stability of lncRNA-0949 through its specific m⁶A sites. HMO6 cells were transfected with control siRNA (siNC) or METTL3 siRNA (siMETTL3) and then left untreated or stimulated with LPS, generating four experimental groups: control (siNC, untreated), LPS (siNC + LPS), control+siMETTL3 (siMETTL3, untreated), and LPS+siMETTL3. **(A)** RNA stability assay. After LPS stimulation, actinomycin D (5 μg/mL) was added, and the relative residual levels of lncRNA-0949 were detected by qPCR at 0, 6, 12, and 24 h (the 0 h value was set as 100%). **(B)** Luciferase reporter assay. Cells were co-transfected with reporter vectors carrying wild-type (WT) or m⁶A site-mutated (Mut; GGACA→GGCCA) lncRNA-0949 3'UTR sequences, along with siNC or siMETTL3 as indicated. Luciferase activity was measured at 0, 6, 12, and 24 h post-treatment. Data are presented as mean ± SD from three independent biological replicates (n = 3). Statistical significance was determined by two-way ANOVA followed by Tukey's post hoc test. Asterisks denote statistical significance (**P < 0.01, ***P < 0.001).

Discussion

Our results define a pathogenic epitranscriptional circuit that sustains neuroinflammation in an in vitro model of sepsis-associated encephalopathy (SAE).^{24,25} Specifically, we establish that inflammatory signalling upregulates the m⁶A methyltransferase METTL3 in microglia. METTL3 then catalyses m⁶A deposition on the long non-coding RNA lncRNA-0949, thereby stabilizing it and driving a sustained pro-inflammatory response (Supplementary Figure 2C). This pathway—LPS → METTL3 → m⁶A–lncRNA-0949 → inflammation—forges a causal chain linking pathogen sensing, RNA modification, non-coding RNA stability and inflammatory phenotype (Supplementary Figure 2D–F),^{26–28} offering a novel molecular framework for understanding SAE pathology.

Our data indicate that METTL3 is a key regulatory molecule in this pathway. In microglia, METTL3 expression increased in a time-dependent manner after LPS stimulation (Figure 1D and E), consistent with its role as an early response gene downstream of TLR4 signaling in immune cells.^{29,30} The functional importance of METTL3 was confirmed by gene knockout experiments, which showed significant reductions in inflammatory cytokine release and oxidative stress markers upon METTL3 depletion (Figure 4C and D, Supplementary Figure 3A). These findings position METTL3 as a molecular switch linking innate immune recognition to downstream inflammatory transcriptome reprogramming.^{27,31} Previous studies have focused more on the role of METTL3 in maintaining microglia homeostasis,^{14,32} while our work is the first to explicitly link its pathological hyperactivation to the neuroinflammatory mechanism of SAE, thus revealing its potential as a therapeutic target for intervention in neuroinflammatory conditions such as SAE.

This study provides a mechanistic explanation for how lncRNA-0949 is regulated. It was found that lncRNA-0949 acts as a direct downstream target of METTL3. Specifically, METTL3 was shown to add an m⁶A modification at a particular site within the 3'UTR of lncRNA-0949 (Figure 2). This modification significantly increased the stability of the lncRNA-0949 transcript (Figure 3A). This stabilizing effect is in line with the known function of m⁶A “reader” proteins like YTHDF and IGF2BPs.^{19,33–35} Conclusive genetic evidence was obtained to confirm the functional requirement of this m⁶A mark. When wild-type lncRNA-0949 was overexpressed, inflammatory responses were intensified. In

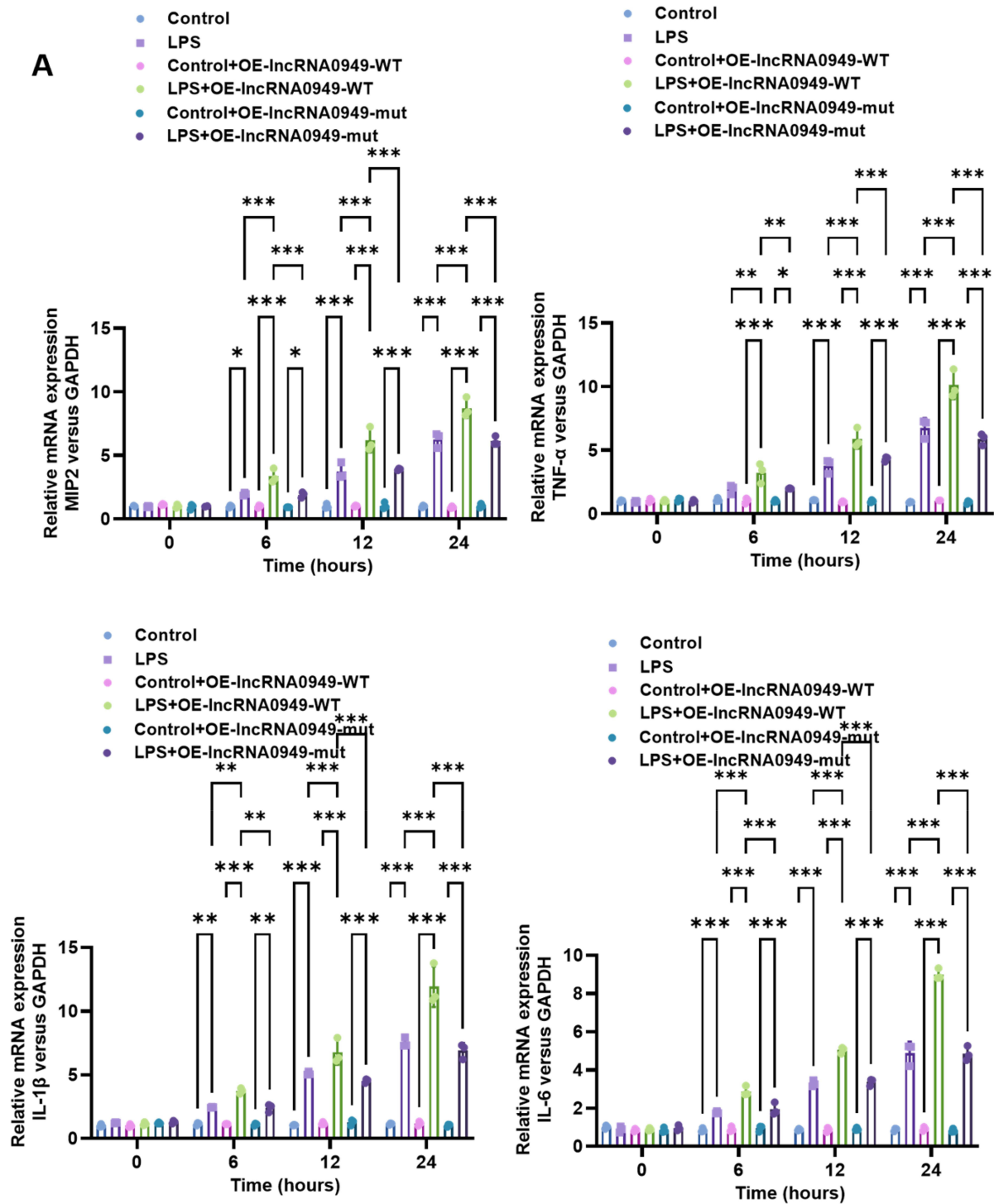


Figure 4 The pro-inflammatory function of lncRNA-0949 strictly depends on its m⁶A modification. **(A and B)** Effects of overexpressing wild-type or m⁶A site-mutated lncRNA-0949 on LPS-induced inflammatory responses at 0, 6, 12, and 24 h. Cells were transfected with wild-type (OE-WT) or m⁶A site-mutated (OE-mut) lncRNA-0949 overexpression vectors and then left untreated or stimulated with LPS. The following six groups are shown: untreated control (Control), OE-WT without LPS (Control+OE-lncRNA0949-WT), OE-mut without LPS (Control+OE-lncRNA0949-mut), LPS stimulation alone (LPS), OE-WT with LPS (LPS+OE-lncRNA0949-WT), and OE-mut with LPS (LPS+OE-lncRNA0949-mut). **(A)** mRNA expression of pro-inflammatory factors (MIP-2, IL-1 β , TNF- α , and IL-6) measured by RT-qPCR. **(B)** Protein concentrations of corresponding cytokines in cell supernatants measured by ELISA. **(C and D)** Effects of METTL3 knockdown on LPS-induced inflammatory responses at 0, 6, 12, and 24 h. HMO6 cells were transfected with control siRNA (siNC) or METTL3 siRNA (siMETTL3) and then left untreated or stimulated with LPS, generating four experimental groups: control (siNC, untreated), LPS (siNC + LPS), control+siMETTL3 (siMETTL3, untreated), and LPS+siMETTL3 (siMETTL3 + LPS). **(C)** mRNA expression of pro-inflammatory factors (MIP-2, IL-1 β , TNF- α , and IL-6) measured by RT-qPCR. **(D)** Protein concentrations of corresponding cytokines measured by ELISA. Data are presented as mean \pm SD from three independent biological replicates (n = 3). Statistical significance was determined by two-way ANOVA followed by Tukey's post hoc test. Asterisks denote statistical significance (*P < 0.05, **P < 0.01, ***P < 0.001).

B

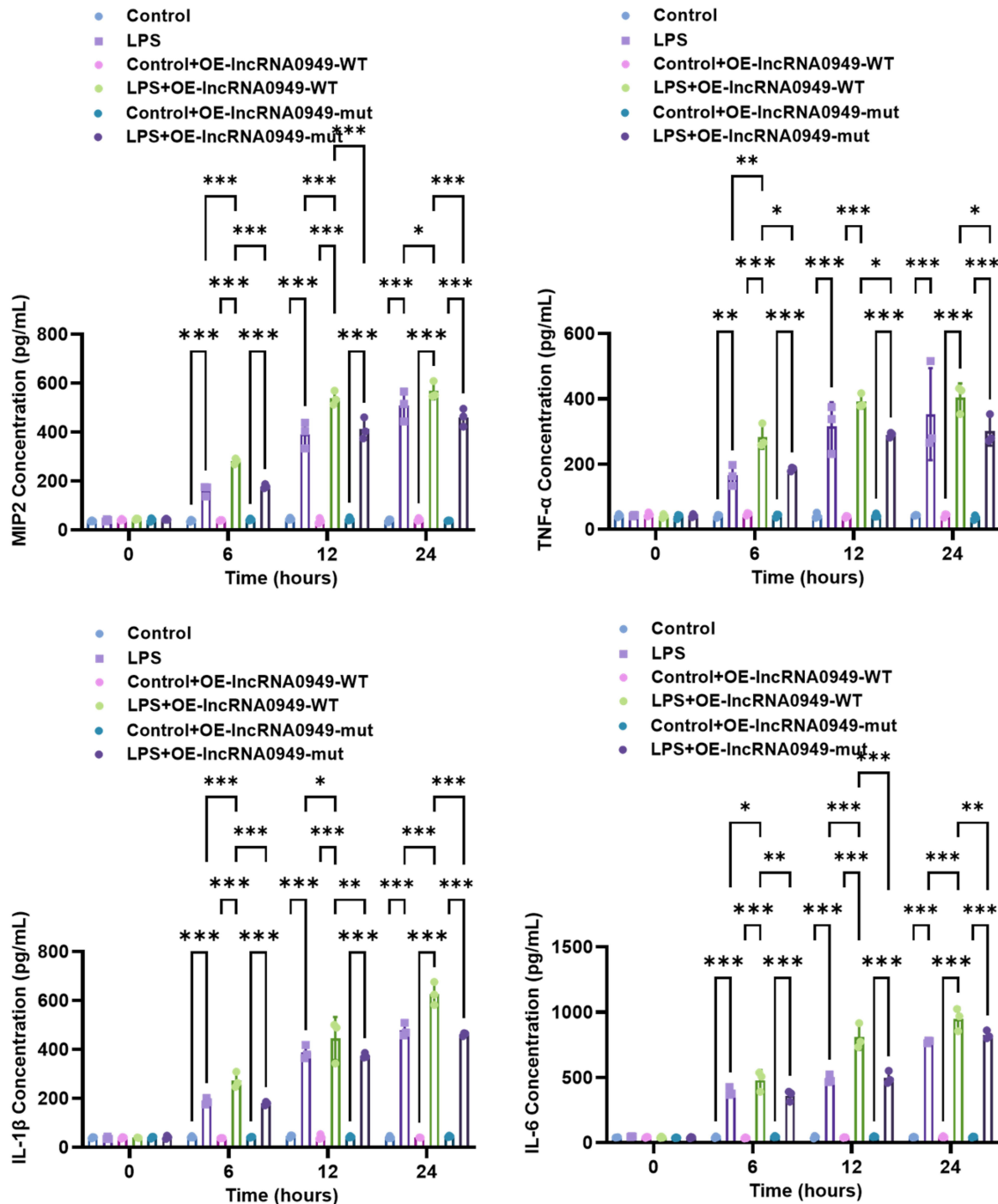


Figure 4 continued.

contrast, overexpression of a mutant form of lncRNA-0949, in which the m⁶A site was disrupted, produced no such effect (Figure 4A and B). Therefore, the m⁶A modification is not merely associated with the lncRNA's function but is a direct cause of it. This chemical modification forms the essential basis for the pro-inflammatory activity of lncRNA-0949. In this way, a direct epitranscriptional regulatory mechanism is established.^{36,37}

Notably, both METTL3 and the m⁶A reader IGF2BP2—which stabilizes modified RNAs—were co-upregulated under inflammatory stress (Supplementary Figure 2E).^{27,38} While direct evidence for IGF2BP2 binding to m⁶A-modified

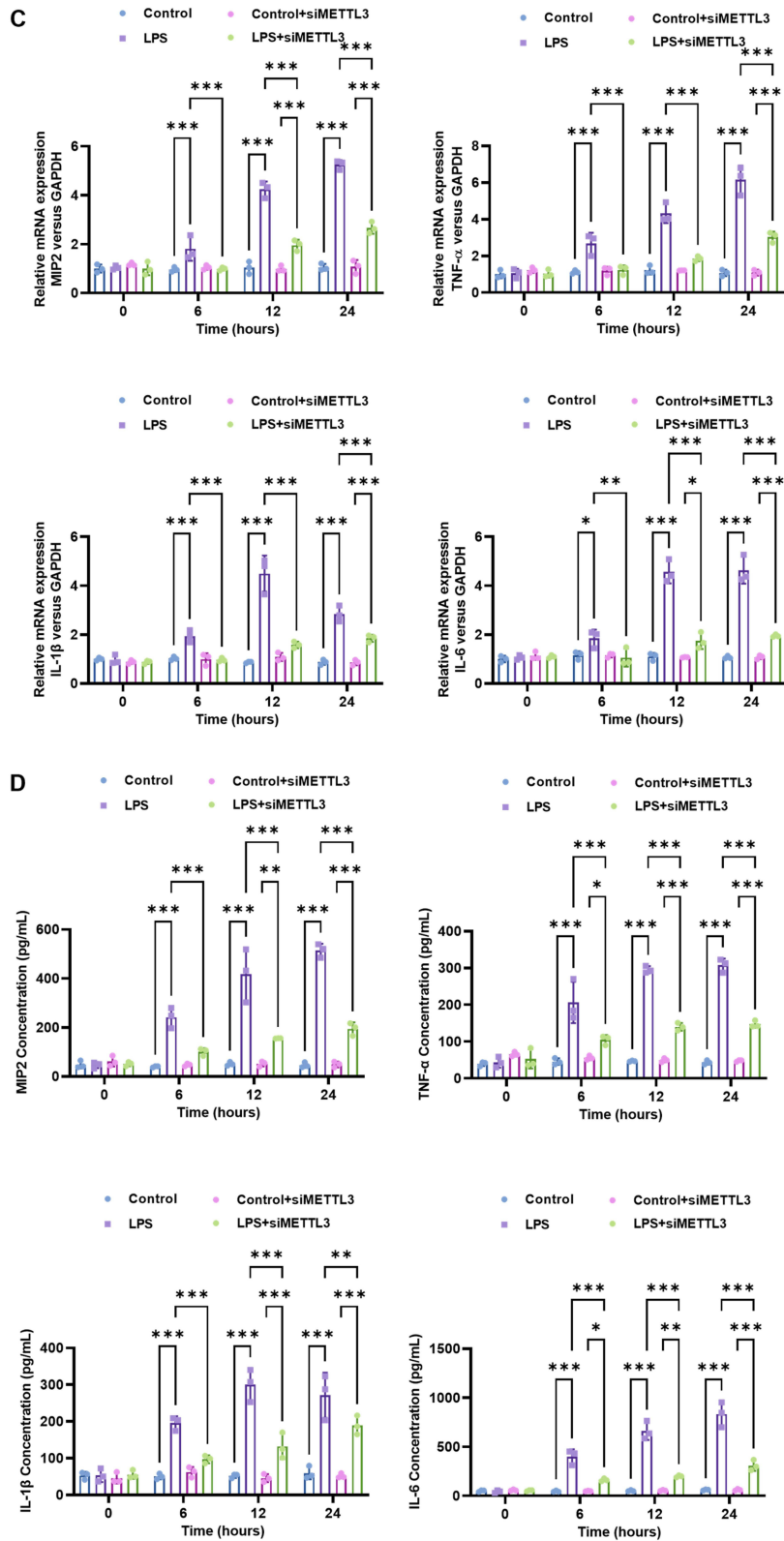


Figure 4 continued.

lncRNA-0949 is currently lacking, their co-upregulation is consistent with a potential functional link. Given their respective catalytic and stabilizing functions^{34,38–40} and the prevalence of feedback in signalling networks,^{41–43} we posit a testable model: that METTL3 and IGF2BP2 may form a positive feedback loop (METTL3 → m⁶A–lncRNA-0949 → IGF2BP2 stabilization → sustained inflammation → METTL3 upregulation). We emphasize that this speculative model requires direct experimental validation, which would provide a novel mechanistic explanation for the self-sustaining nature of pathological neuroinflammation.

While this work defines a core epitranscriptional pathway linking METTL3 to lncRNA-0949 in microglial inflammation, several important questions remain. First, the precise mechanism by which m⁶A-modified lncRNA-0949 executes its pro-inflammatory program requires resolution. Although our data demonstrate that the m⁶A site is essential for lncRNA-0949 function, the molecular mode of action—whether it functions as a competing endogenous RNA (ceRNA) sequestering regulatory microRNAs (eg, miR-146a, miR-155),^{44–46} or as a scaffold assembling components of signalling hubs such as NF-κB or the NLRP3 inflammasome^{47,48}—remains speculative. RNA pulldown coupled with mass spectrometry could identify its interacting protein partners, while luciferase reporters bearing predicted miRNA binding sites could test the ceRNA hypothesis. Second, while METTL3 knockdown and lncRNA-0949 overexpression experiments collectively implicate lncRNA-0949 as a downstream effector of METTL3, direct genetic manipulation—specifically, lncRNA-0949 knockdown and rescue with WT versus mutant constructs—would further solidify causality. Third, although our *in vitro* model establishes cell-autonomous function in microglia, the operational logic and necessity of this axis within the integrated neural circuitry of an intact brain—involving cross-talk with neurons and astrocytes—demands validation in SAE animal models.^{49,50} Finally, translation to human pathology will require profiling METTL3 activity and m⁶A-modified lncRNA-0949 in patient samples, where correlation with clinical severity could validate their pathogenic role and evaluate their potential as biomarkers or therapeutic guides.^{51–54}

In summary, this work delineates a pathogenic epitranscriptional circuit—the METTL3–m⁶A–lncRNA-0949 axis—that drives and sustains neuroinflammation in an *in vitro* model of SAE, providing a mechanistic framework with potential relevance to the human condition.

Conclusion

Our research delineates a pathogenic mechanism in an *in vitro* model of sepsis-associated encephalopathy (SAE), in which inflammatory signalling upregulates the m⁶A methyltransferase METTL3 to catalyse site-specific modification of the long non-coding RNA lncRNA-0949, whose pro-inflammatory function we identify for the first time, thereby stabilizing it and propagating inflammation. By establishing a complete causal chain from environmental stimulus → epitranscriptomic writer → this functionally uncharacterized lncRNA → inflammatory phenotype, our findings bridge discrete levels of regulation and nominate METTL3-mediated m⁶A deposition as a potential therapeutic target for mitigating aberrant microglial activation in neuroinflammatory conditions such as SAE.

Data Sharing Statement

The experimental data that support the results presented in this article are available from the corresponding author upon reasonable request.

Author Contributions

Xing Zeng: Conceptualization, Investigation, Methodology, Formal analysis, Writing – original draft, Visualization, Writing – review & editing. Yi-An Zhan: Supervision, Funding acquisition, Project administration, Resources, Writing – review & editing. Xiao-Juan Luo: Validation, Data curation, Software, Writing – review & editing. Zhen-Ze Zhang: Investigation, Resources, Validation, Writing – review & editing. Jia-Li Lu: Data curation, Writing – review & editing. All authors gave final approval of the version to be published; have agreed on the journal to which the article has been submitted; and agree to be accountable for all aspects of the work.

Funding

The authors thank the National Natural Science Foundation of China (82060345) for financial support.

Disclosure

No competing interests are declared by the authors.

References

- Molnár L, Fülesdi B, Németh N, Molnár C. Sepsis-associated encephalopathy: a review of literature. *Neurol India*. 2018;66(2):352–361. doi:10.4103/0028-3886.227299
- Zhang QH, Sheng ZY, Yao YM. Septic encephalopathy: when cytokines interact with acetylcholine in the brain. *Military Med Res*. 2014;1:20. doi:10.1186/2054-9369-1-20
- Ou G, Che J, Dong J, et al. Methylene blue targets PHD3 expression in murine microglia to mitigate lipopolysaccharide-induced neuroinflammation and neurocognitive impairments. *Int Immunopharmacol*. 2023;120:110349. doi:10.1016/j.intimp.2023.110349
- Vejuh A. Cell death, inflammation and oxidative stress in neurodegenerative diseases: mechanisms and cytoprotective molecules. *Int J Mol Sci*. 2021;22(24):13657. doi:10.3390/ijms222413657
- Garaschuk O, Verkhratsky A. Physiology of Microglia. *Method Mol Biol*. 2019;2034:27–40. doi:10.1007/978-1-4939-9658-2_3
- Sopic M, Robinson EL, Emanuelli C, et al. Integration of epigenetic regulatory mechanisms in heart failure. *Basic Res Cardiol*. 2023;118(1):16. doi:10.1007/s00395-023-00986-3
- Zuo X, Chen Z, Gao W, et al. m6A-mediated upregulation of LINC00958 increases lipogenesis and acts as a nanotherapeutic target in hepatocellular carcinoma. *J Hematol Oncol*. 2020;13(1):5. doi:10.1186/s13045-019-0839-x
- Han SH, Choe J. Diverse molecular functions of m(6)A mRNA modification in cancer. *Exp Mol Med*. 2020;52(5):738–749. doi:10.1038/s12276-020-0432-y
- Xu W, Zhang L, Geng Y, Liu Y, Zhang N. Long noncoding RNA GAS5 promotes microglial inflammatory response in Parkinson's disease by regulating NLRP3 pathway through sponging miR-223-3p. *Int Immunopharmacol*. 2020;85:106614. doi:10.1016/j.intimp.2020.106614
- Knowling S, Morris KV. Non-coding RNA and antisense RNA. Nature's trash or treasure? *Biochimie*. 2011;93(11):1922–1927. doi:10.1016/j.biochi.2011.07.031
- Liu L, Zhou T, Li T, Liang Z, Luo X. LncRNA DLX6-AS1 promotes microglial inflammatory response in Parkinson's disease by regulating the miR-223-3p/NRP1 axis. *Behav Brain Res*. 2022;431:113923. doi:10.1016/j.bbr.2022.113923
- Rinn JL, Chang HY. Genome regulation by long noncoding RNAs. *Annu Rev Biochem*. 2012;81:145–166. doi:10.1146/annurev-biochem-051410-092902
- Huang H, Weng H, Sun W, et al. Recognition of RNA N(6)-methyladenosine by IGF2BP proteins enhances mRNA stability and translation. *Nat Cell Biol*. 2018;20(3):285–295. doi:10.1038/s41556-018-0045-z
- Wen L, Sun W, Xia D, Wang Y, Li J, Yang S. The m6A methyltransferase METTL3 promotes LPS-induced microglia inflammation through TRAF6/NF- κ B pathway. *Neuroreport*. 2022;33(6):243–251. doi:10.1097/wnr.0000000000001550
- Tsai MC, Manor O, Wan Y, et al. Long noncoding RNA as modular scaffold of histone modification complexes. *Science*. 2010;329(5992):689–693. doi:10.1126/science.1192002
- Saadth MJ, Allela OQB, Al-Hussainy AF, et al. Exosomal non-coding RNAs: gatekeepers of inflammation in autoimmune disease. *J Inflamm*. 2025;22(1):18. doi:10.1186/s12950-025-00443-z
- Ye Y, He X, Lu F, et al. A lincRNA-p21/miR-181 family feedback loop regulates microglial activation during systemic LPS- and MPTP- induced neuroinflammation. *Cell Death Dis*. 2018;9(8):803. doi:10.1038/s41419-018-0821-5
- Li Z, Chao TC, Chang KY, et al. The long noncoding RNA THRIL regulates TNF α expression through its interaction with hnRNPL. *Proc Natl Acad Sci USA*. 2014;111(3):1002–1007. doi:10.1073/pnas.1313768111
- Qian X, Li X, Zheng Z, et al. METTL3 orchestrates cancer progression by m(6)A-dependent modulation of oncogenic lncRNAs. *Int J Biol Macromol*. 2025;310(Pt 3):143299. doi:10.1016/j.ijbiomac.2025.143299
- Tang F, Tian LH, Zhu XH, Yang S, Zeng H, Yang YY. METTL3-mediated m6A modification enhances lncRNA H19 stability to promote endothelial cell inflammation and pyroptosis to aggravate atherosclerosis. *FASEB J*. 2024;38(20):e70090. doi:10.1096/fj.202401337RR
- Livak KJ, Schmittgen TD. Analysis of relative gene expression data using real-time quantitative PCR and the 2(-Delta Delta C(T)) Method. *Methods*. 2001;25(4):402–408. doi:10.1006/meth.2001.1262
- Li Y, Huang L, Fang M, et al. The flip side of the coin: METTL3 serves as a novel cellular senescence accelerator via negative regulation of ITGA9. *Aging Dis*. 2025;17(2):1034–1051. doi:10.14336/ad.2024.1715
- Anbazzhagan AN, Priyamvada S, Kumar A, et al. Translational repression of SLC26A3 by miR-494 in intestinal epithelial cells. *Am J Physiol Gastrointest Liver Physiol*. 2014;306(2):G123–31. doi:10.1152/ajpgi.00222.2013
- Deng J, Chen X, Chen A, Zheng X. m(6)A RNA methylation in brain injury and neurodegenerative disease. *Front Neurol*. 2022;13:995747. doi:10.3389/fneur.2022.995747
- Livneh I, Moshitch-Moshkovitz S, Amariglio N, Rechavi G, Dominissini D. The m(6)A epitranscriptome: transcriptome plasticity in brain development and function. *Nat Rev Neurosci*. 2020;21(1):36–51. doi:10.1038/s41583-019-0244-z
- Wu X, Liu H, Wang J, et al. The m(6)A methyltransferase METTL3 drives neuroinflammation and neurotoxicity through stabilizing BATF mRNA in microglia. *Cell Death Differ*. 2025;32(1):100–117. doi:10.1038/s41418-024-01329-y
- Dong A, Zhang P, Yang F, Wang Y, Liu H. ADAP-METTL3 modulates the inflammatory responses of macrophages via m(6)A modification of Spry1. *Cell Death Dis*. 2025;16(1):708. doi:10.1038/s41419-025-08008-x
- Wang J, Yan S, Lu H, Wang S, Xu D. METTL3 attenuates LPS-induced inflammatory response in macrophages via NF- κ B signaling pathway. *Mediat Inflamm*. 2019;2019:3120391. doi:10.1155/2019/3120391
- Miller C, Ealy A, Gregory A, et al. Pathological α -synuclein dysregulates epitranscriptomic writer METTL3 to drive neuroinflammation in microglia. *Cell Rep*. 2025;44(5):115618. doi:10.1016/j.celrep.2025.115618
- Zhang F, Ran Y, Tahir M, Li Z, Wang J, Chen X. Regulation of N6-methyladenosine (m6A) RNA methylation in microglia-mediated inflammation and ischemic stroke. *Front Cell Neurosci*. 2022;16:955222. doi:10.3389/fncel.2022.955222

31. Wu Q, Zou Q, Long S, Deng H, Cui Y. METTL3 promotes oxidative stress and inflammation in myoblasts during chronic kidney disease related sarcopenia through the TLR4 NF- κ B pathway. *Microbiol Immunol.* 2025;69(12):608–618. doi:10.1111/1348-0421.70014
32. Wang J, Sha Y, Sun T. m(6)A modifications play crucial roles in glial cell development and brain tumorigenesis. *Front Oncol.* 2021;11:611660. doi:10.3389/fonc.2021.611660
33. Xiao R, Lu X, Huang F, et al. METTL3-mediated m6A methylation on lncRNA H19 inhibits intrahepatic cholangiocarcinoma progression through PPAR γ downregulation. *Int J Bio Sci.* 2025;21(14):6062–6080. doi:10.7150/ijbs.120413
34. Bian Y, Xu S, Gao Z, et al. m(6)A modification of lncRNA ABHD11-AS1 promotes colorectal cancer progression and inhibits ferroptosis through TRIM21/IGF2BP2/FOXO1 positive feedback loop. *Cancer Lett.* 2024;596:217004. doi:10.1016/j.canlet.2024.217004
35. Liu HT, Zou YX, Zhu WJ, et al. lncRNA THAP7-AS1, transcriptionally activated by SP1 and post-transcriptionally stabilized by METTL3-mediated m6A modification, exerts oncogenic properties by improving CUL4B entry into the nucleus. *Cell Death Differ.* 2022;29(3):627–641. doi:10.1038/s41418-021-00879-9
36. Olazagoitia-Garmendia A, Rojas-Márquez H, Sebastian-delaCruz M, et al. m(6)A methylated long noncoding RNA LOC339803 regulates intestinal inflammatory response. *Adv Sci.* 2024;11(13):e2307928. doi:10.1002/advs.202307928
37. Liu P, Zhang B, Chen Z, et al. m(6)A-induced lncRNA MALAT1 aggravates renal fibrogenesis in obstructive nephropathy through the miR-145/FAK pathway. *Aging.* 2020;12(6):5280–5299. doi:10.18632/aging.102950
38. Zhu C, Li R, You X, et al. m6A reader IGF2BP2-stabilized lncRNA LHX1-DT inhibits renal cell carcinoma (RCC) cell proliferation and invasion by sponging miR-590-5p. *NPJ Precision Oncol.* 2025;9(1):193. doi:10.1038/s41698-025-00958-x
39. Kim SY, Ha JW, Na MJ, et al. Oncogenic function of growth arrest-specific transcript 5 by competing with miR-423-3p to regulate SMARCA4 in hepatocellular carcinoma. *Exp Mol Med.* 2025;57(6):1164–1176. doi:10.1038/s12276-025-01459-4
40. Chi D, Li F, Wang Z. Mechanisms of methyltransferase-like 3-mediated microglial pyroptosis in sepsis-associated encephalopathy. *Neuroreport.* 2025;36(16):949–959. doi:10.1097/wnr.0000000000002215
41. Dubey SR, Turnbull C, Pandey A, et al. Molecular mechanisms and regulation of inflammasome activation and signaling: sensing of pathogens and damage molecular patterns. *Cell Mol Immunol.* 2025;22(11):1313–1344. doi:10.1038/s41423-025-01354-y
42. Chen F, Jiang G, Liu H, et al. Melatonin alleviates intervertebral disc degeneration by disrupting the IL-1 β /NF- κ B-NLRP3 inflammasome positive feedback loop. *Bone Res.* 2020;8:10. doi:10.1038/s41413-020-0087-2
43. Shinohara H, Behar M, Inoue K, et al. Positive feedback within a kinase signaling complex functions as a switch mechanism for NF- κ B activation. *Science.* 2014;344(6185):760–764. doi:10.1126/science.1250020
44. Nie T, Zhang C, Zhang G, et al. lncRNA CALML3-AS1 regulates chondrocyte apoptosis by acting as a sponge for miR-146a. *Autoimmunity.* 2021;54(6):336–342. doi:10.1080/08916934.2021.1943663
45. Huang SF, Zhao G, Peng XF, Ye WC. The Pathogenic Role of Long Non-coding RNA H19 in Atherosclerosis via the miR-146a-5p/ANGPTL4 Pathway. *Front Cardiovasc Med.* 2021;8:770163. doi:10.3389/fcvm.2021.770163
46. Sun W, Ma M, Yu H, Yu H. Inhibition of lncRNA X inactivate-specific transcript ameliorates inflammatory pain by suppressing satellite glial cell activation and inflammation by acting as a sponge of miR-146a to inhibit Na(v) 1.7. *J Cell Biochem.* 2018;119(12):9888–9898. doi:10.1002/jcb.27310
47. Ye M, Wang C, Zhu J, et al. An NF- κ B-responsive long noncoding RNA, PINT, regulates TNF- α gene transcription by scaffolding p65 and EZH2. *FASEB J.* 2021;35(9):e21667. doi:10.1096/fj.202002263R
48. Menon MP, Hua KF. The long non-coding RNAs: paramount regulators of the NLRP3 inflammasome. *Front Immunol.* 2020;11:569524. doi:10.3389/fimmu.2020.569524
49. Zeng QQ, Qi Y, Yu H, et al. Pharmacological inhibition of the cGAS-STING pathway suppresses microglia pyroptosis in sepsis-associated encephalopathy. *J Neuroinflamm.* 2025;22(1):176. doi:10.1186/s12974-025-03507-2
50. Fu Q, Zhang YB, Shi CX, et al. GSDMD/Drp1 signaling pathway mediates hippocampal synaptic damage and neural oscillation abnormalities in a mouse model of sepsis-associated encephalopathy. *J Neuroinflamm.* 2024;21(1):96. doi:10.1186/s12974-024-03084-w
51. Wu D, Spencer CB, Ortoga L, Zhang H, Miao C. Histone lactylation-regulated METTL3 promotes ferroptosis via m6A-modification on ACSL4 in sepsis-associated lung injury. *Redox Biol.* 2024;74:103194. doi:10.1016/j.redox.2024.103194
52. Li F, Zhang Y, Peng Z, Wang Y, Zeng Z, Tang Z. Diagnostic, clustering, and immune cell infiltration analysis of m6A regulators in patients with sepsis. *Sci Rep.* 2023;13(1):2532. doi:10.1038/s41598-022-27039-4
53. Wei XB, Jiang WQ, Zeng JH, et al. Exosome-derived lncRNA NEAT1 exacerbates sepsis-associated encephalopathy by promoting ferroptosis through regulating miR-9-5p/TFRC and GOT1 axis. *Mol Neurobiol.* 2022;59(3):1954–1969. doi:10.1007/s12035-022-02738-1
54. Wang H, Wang Q, Chen J, Chen C. Association among the gut microbiome, the serum metabolomic profile and RNA m(6)A methylation in sepsis-associated encephalopathy. *Front Genet.* 2022;13:859727. doi:10.3389/fgene.2022.859727